



## Broadband impedance-matched electromagnetic structured ferrite composite in the megahertz range

L. Parke, I. J. Youngs, A. P. Hibbins, and J. R. Sambles

Citation: [Applied Physics Letters](#) **104**, 221905 (2014); doi: 10.1063/1.4881186

View online: <http://dx.doi.org/10.1063/1.4881186>

View Table of Contents: <http://scitation.aip.org/content/aip/journal/apl/104/22?ver=pdfcov>

Published by the [AIP Publishing](#)

---

### Articles you may be interested in

[Heavily loaded ferrite-polymer composites to produce high refractive index materials at centimetre wavelengths](#)  
APL Mat. **1**, 042108 (2013); 10.1063/1.4824039

[Ultrabroad bandwidth and matching characteristics for spinel ferrite composites with flaky fillers](#)  
J. Appl. Phys. **108**, 063927 (2010); 10.1063/1.3485809

[Dielectric and magnetic properties of 0.4 PZT + 0.6 NiCuZn -ferrite composites modified with P 2 O 5 – Co 2 O 3](#)  
J. Appl. Phys. **107**, 09E309 (2010); 10.1063/1.3360197

[Influential parameters on electromagnetic properties of nickel–zinc ferrites for antenna miniaturization](#)  
J. Appl. Phys. **107**, 09A518 (2010); 10.1063/1.3356235

[Ferromagnetic resonance and dielectric and magnetic properties of pure and diluted ferrites in millimeter waves](#)  
J. Appl. Phys. **105**, 07A503 (2009); 10.1063/1.3059611

---

A promotional banner for COMSOL 5.0. The background is a light gray grid with several colorful, flowing lines in shades of blue, green, yellow, and red. The text 'Build and Run Simulation Apps with COMSOL 5.0' is centered in a dark red, serif font. Below the text is a dark red button with a white play icon and the text 'SEE HOW'. In the bottom right corner, the COMSOL logo is displayed, consisting of three red squares followed by the word 'COMSOL' in a dark red, sans-serif font.

## Broadband impedance-matched electromagnetic structured ferrite composite in the megahertz range

L. Parke,<sup>1</sup> I. J. Youngs,<sup>2</sup> A. P. Hibbins,<sup>1</sup> and J. R. Sambles<sup>1</sup>

<sup>1</sup>*Electromagnetic and Acoustic Materials Group, Department of Physics and Astronomy, University of Exeter, Stocker Road, Exeter, Devon EX4 4QL, United Kingdom*

<sup>2</sup>*DSTL, Salisbury, Wiltshire SP4 0JQ, United Kingdom*

(Received 26 February 2014; accepted 21 May 2014; published online 3 June 2014)

A high refractive-index structured ferrite composite is designed to experimentally demonstrate broadband impedance matching to free-space. It consists of an array of ferrite cubes that are anisotropically spaced, thereby allowing for independent control of the effective complex permeability and permittivity. Despite having a refractive index of 9.5, the array gives less than 1% reflection and over 90% transmission of normally incident radiation up to 70 MHz for one of the orthogonal linear polarisations lying in a symmetry plane of the array. This result presents a route to the design of MHz-frequency ferrite composites with bespoke electromagnetic parameters for antenna miniaturisation. © 2014 AIP Publishing LLC. [<http://dx.doi.org/10.1063/1.4881186>]

When matching of the complex wave impedance occurs at an interface between two different media, the reflection from the interface is zero, allowing for complete power transmission. To be able to obtain this impedance match (zero insertion loss) would stimulate advances in the practical aspect of transformation optics, stealth technology, antireflection coatings, and antenna miniaturisation.<sup>1</sup> One requires

$$\frac{\tilde{\mu}_{r1}}{\tilde{\epsilon}_{r1}} = \frac{\tilde{\mu}_{r2}}{\tilde{\epsilon}_{r2}}, \quad (1)$$

to ensure no reflection for normal incidence radiation. In these equations,  $\tilde{\mu}_r = \mu'_r + i\mu''_r$  and  $\tilde{\epsilon}_r = \epsilon'_r + i\epsilon''_r$  are the relative complex permeability and permittivity, respectively, where the subscripts identify the media either side of the interface. For normal incidence, from free space, the complex relative permittivity and permeability of the material must be equal. Such impedance matching conditions are difficult to achieve since they require electromagnetic material properties that are not widely found in nature.

It is the focus of this study to design, construct and characterise a broadband high-index but impedance-matched medium to air. This requires the development and utilisation of bulk materials with equal and identically dispersive complex permittivity and permeability. While many naturally occurring materials have high permittivity values, there are few with similarly high permeabilities. One such class of materials are the ferrites, which have high and reasonably non-dispersive permeability. These are used in many applications, such as telecommunications and antenna systems.<sup>2</sup> Many ferrites also simultaneously have a non-dispersive and a high permittivity in the MHz and low GHz range since they are comprised of semiconducting grains encapsulated by insulating oxide barriers<sup>3</sup> that leads to charge separation and high polarisability of the grains. However, in order to equalise  $\tilde{\mu}_r$  and  $\tilde{\epsilon}_r$  some material or chemical modification has conventionally been required.

Previous work has demonstrated broadband impedance matching using nano-sized ferrite particles sintered into a solid sample.<sup>4</sup> Although  $\mu'_r$  and  $\epsilon'_r$  cannot be controlled independently, impedance matching between 100–500 MHz,

with a refractive index of 4.8, is achieved. Kong, Li, Lin, and Gan<sup>5</sup> showed that it is possible to independently control  $\mu'_r$  of a 50% vol. Ni<sub>0.95-x</sub>Zn<sub>x</sub>Co<sub>0.05</sub>Mn<sub>0.02</sub> ferrite epoxy composite by varying the proportion of zinc in the ferrite, with impedance matching (at a refractive index of 6.5) achieved up to 30 MHz. More recently, impedance matching has been achieved by controlling the sintering temperature of a NiCuZn ferrite finding equality of  $\mu'_r$  and  $\epsilon'_r$  at a value of 11.8 from 10–100 MHz.<sup>6</sup> However, while the sintering process altered both  $\mu'_r$  and  $\epsilon'_r$  simultaneously, independent control of these parameters was not possible. Controlling  $\mu'_r$  and  $\epsilon'_r$  of Bi-Co-Ti substituted M-type ferrite has also been demonstrated by controlling the sintering temperature to between 900 and 950 °C.<sup>7</sup> Although  $\mu'_r$  and  $\epsilon'_r$  were matched at a value of 24 over the frequency range of 10–200 MHz, the method does not allow for the extra degree of freedom that our structured composite provides. The method described here of structuring bulk materials allows matching the impedance in a simple manner although it must be emphasised that it is only for one incident polarisation.

Impedance matching does not necessarily require the use of ferrimagnetic materials. It can also be realised resonantly via artificial magnetism or by implementing transmission line networks.<sup>8</sup> An example of a resonant impedance-matched metamaterial is in Ref. 9, where a configuration of two metallic resonators that couple separately to electric and magnetic fields, where impedance matching is achieved by tuning separately both resonant frequencies. Although this metamaterial is impedance matched at a high frequency (~11 GHz), it is a resonant effect, and therefore narrowband. Kim and Park<sup>10</sup> have designed an ultra-thin ( $\lambda/25$ ) antireflection coating by employing a pair of dispersive metamaterial layers on the face of a slab of Teflon. The approach considered in our present work is to incorporate a sub-wavelength structure into a bulk ferrite composite to create a structured ferrite composite with a high refractive index, impedance matched over a broad band. It is a concept similar to that considered by Matsumoto and Miyata in 1997 in order to reduce reflections from a resonant absorber<sup>11</sup> by reducing the effective permittivity, without greatly

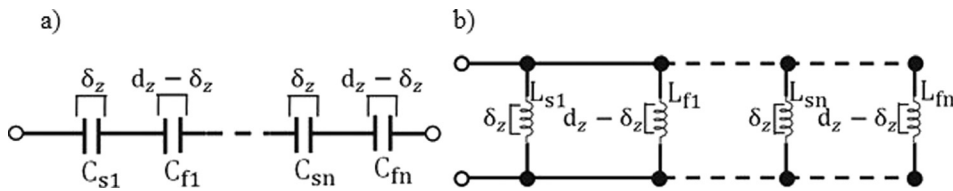


FIG. 1. Equivalent electrical circuits for structured ferrite composite with (a) capacitors representing the permittivity and (b) inductors representing the permeability.

perturbing its permeability and magnetic loss. Consider an infinite stack of ferrite composite, for an electric field normal to the slab plane it is trivial to show that for an infinite stack, the effective relative permittivity,  $\epsilon'_{\text{eff}}$ , is given by

$$\frac{1}{\epsilon'_{\text{eff}}} = \frac{1}{\epsilon'_f} + \frac{\delta_z}{d_z} \left( \frac{1}{\epsilon'_s} - \frac{1}{\epsilon'_f} \right). \quad (2)$$

Here,  $\epsilon'_s$  is the relative permittivity of the spacer material,  $\epsilon'_f$  is the relative permittivity of the ferrite composite,  $d_z$  is the combined thickness of a slab and spacer material, and  $\delta_z$  is the thickness of the low permittivity spacer only. It is clear that if  $\epsilon'_f \gg \epsilon'_s$  small changes in  $\delta_z$  will greatly alter  $\epsilon'_{\text{eff}}$ .

By contrast since the magnetic induction lies in the plane of the slabs, the effective relative permeability,  $\mu'_{\text{eff}}$ , is given by

$$\mu'_{\text{eff}} = \mu'_f + \frac{\delta_z}{d_z} (\mu'_s - \mu'_f). \quad (3)$$

Here,  $\mu'_s$  is the relative permeability of the spacer material and  $\mu'_f$  is the relative permeability of the composite. The equivalent electrical circuits for describing Eqs. (2) and (3) are shown in Figures 1(a) and 1(b). Both circuits represent an infinite stack of alternating spacer material with electromagnetic properties  $\epsilon_s$  and  $\mu_s$  and ferrite composite with electromagnetic properties  $\epsilon_f$  and  $\mu_f$ .  $C_s$  and  $C_f$  correspond to the capacitances of the spacer and ferrite composite while  $L_s$  and  $L_f$  are their inductances.

This structuring thus allows a degree of independent control (for one polarisation) of the relative permittivities and permeabilities by varying the low index dielectric spacer thickness: Matsumoto and Miyata<sup>11</sup> obtained  $\mu'_{\text{eff}} = 3$  and  $\epsilon'_{\text{eff}} = 10$  at 3 GHz for their layered material (the relative permittivity of the unstructured material was determined to be  $\sim 200$  at the same frequency). Whilst the layering of the material did not make  $\epsilon'_r$  and  $\mu'_r$  equal, the performance of the absorber was improved: the predicted minimum reflection of the absorber at normal incidence on resonance was reduced from  $\sim 25\%$  (at  $\sim 300$  MHz) when unlayered to  $\sim 0.1\%$  (at  $\sim 3$  GHz) when layered.

For the alternate case of the propagation vector and electric field vector lying in the plane of the layers,  $\mu'_{\text{eff}}$  and  $\epsilon'_{\text{eff}}$  obey the following dependence on  $\delta_z$ :

$$\frac{1}{\mu'_{\text{eff}}} = \frac{1}{\mu'_f} + \frac{\delta_z}{d_z} \left( \frac{1}{\mu'_s} - \frac{1}{\mu'_f} \right), \quad (4)$$

$$\epsilon'_{\text{eff}} = \epsilon'_f + \frac{\delta_z}{d_z} (\epsilon'_s - \epsilon'_f), \quad (5)$$

i.e., the dependencies of  $\mu'_{\text{eff}}$  and  $\epsilon'_{\text{eff}}$  on  $\delta_z$  reverse their roles for the orthogonal polarisation. This simple slab model is an excellent approximation that can be applied to more

complicated systems such as anisotropic arrays of columns or cubes provided the thickness of any dielectric spacers in directions perpendicular to  $\delta_z$  are small compared to the cube sizes and  $\delta_z$ .

In our present study, we design and experimentally demonstrate a structured ferrite composite of refractive index  $\sim 9.5$  that is impedance matched to free space for frequencies up to 70 MHz for one of the orthogonal linear polarisations collinear with the axes of the array. In addition, our experimental results demonstrate that a 50 mm length of this structure transmits more than 90% of the incident power up to 70 MHz, and maintains a reflection coefficient of less than 0.3% up to 300 MHz, despite becoming absorbing. The structure is comprised of a commercially available sintered Manganese Zinc ferrite ( $\text{Mn}_{0.8}\text{Zn}_{0.2}\text{Fe}_2\text{O}_4$ ) powder supplied by MagDev Ltd (UK) manufactured into a composite with standard polytetrafluoroethylene (PTFE) powder chosen as the matrix material. The MnZn ferrite and PTFE powders were mixed together with a ferrite volume of 70% and pressed into samples using a steel mould at 55 MPa for 300 s to produce  $1 \times 1 \times 1$  cm cubic ferrite composite elements.<sup>12</sup> Two  $6 \times 5$  layers of cubes, with each cube spaced in the  $x$ - and  $y$ -directions by double sided polyester adhesive tape of thickness 0.1 mm, were fabricated (Figure 2). Each of these planar arrays of cubes were in turn positioned in a calibrated stripline to fill the void between the central signal line, and one of the two symmetrically positioned ground planes. The width of signal line is chosen to maintain 50  $\Omega$  in an unloaded stripline, optimised with a ground-plane–signal-line gap equal to the height of the cubes plus spacers. Each structured slab (5 unit cells) is much wider than the signal line, and hence its response will be indistinguishable from a sample of infinite extent in the  $y$ -direction (Figure 3). The two ground planes above and below the cube arrays replicate the response of an infinitely repeat period ( $z$ -direction) structured slab. The complex reflection and transmission coefficients (S-parameters) of the loaded stripline are recorded as a function of frequency, and the effective, complex permittivity, and permeability are

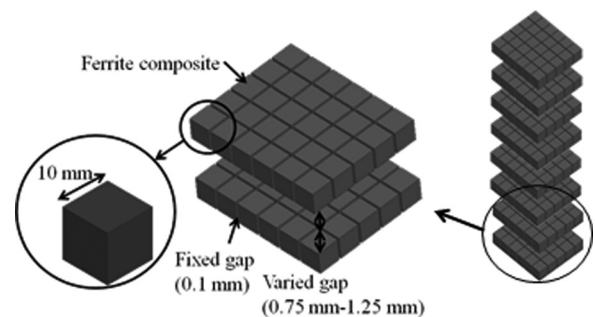


FIG. 2. Anisotropic array of cubes comprised of ferrite composite material. The cubes are spaced in the  $x$  and  $y$ -directions by adhesive tape ( $\delta_x = \delta_y = 0.1$  mm) and in the  $z$ -direction from the ground plane and signal line using polyester film ( $\delta_z = 2 \times 0.75$  mm to  $2 \times 1.25$  mm).

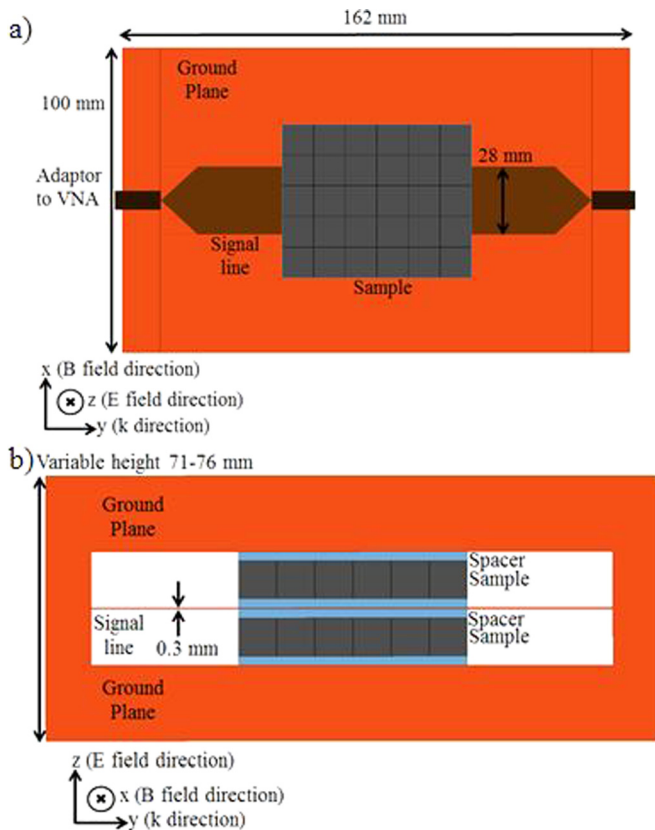


FIG. 3. Schematic of the stripline set up containing the sample and Teflon spacers from (a) side on view and (b) a top down cross section. The stripline is connected to a Vector Network Analyser (VNA) (b).

obtained using the Nicholson, Ross, Weir (NRW) extraction method.<sup>13,14</sup> The effective electromagnetic parameters of this structured design were recorded using polyester spacers between 0.75 mm and 1.25 mm in the  $z$  direction and the impedance matching condition sought.

It is first necessary to determine the complex permittivity and permeability of the bulk ferrite composite material, 70% vol. MnZn ferrite and 30% vol. PTFE (Figure 4). A trade-off between high values of  $\tilde{\mu}_r$  and  $\tilde{\epsilon}_r$  and the brittleness of heavily loaded composites resulted in a 70% vol. ferrite composite being chosen. The values of  $\mu'_r$  and  $\epsilon'_r$  remain approximately constant, while  $\mu''_r$  and  $\epsilon''_r$  remain relatively small from 10 MHz to 100 MHz. The high  $\mu'_r$  of the ferrite

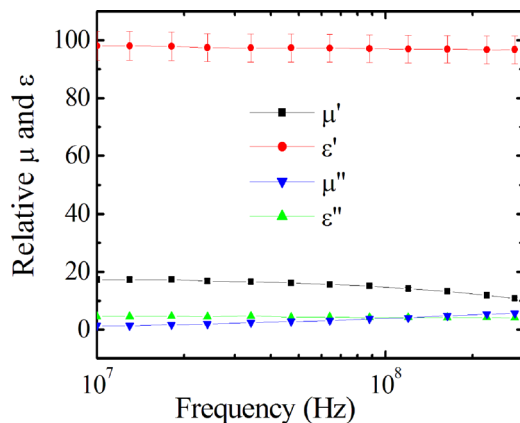


FIG. 4. Frequency dispersion of the complex relative permeability and permittivity of the 70% vol. ferrite and 30% vol. PTFE composite.

material at low frequencies arises from two separate contributions: gyromagnetic spin precession and domain wall motion.<sup>15</sup> Although the resonant frequency associated with these phenomena occurs at approximately 300 MHz,  $\mu'_r$  starts to rise significantly above 70 MHz which sets an upper limit to the impedance matching, even though both  $\mu'_r$  and  $\epsilon'_r$  for this bulk ferrite remain large and frequency independent up to 100 MHz.

In order to determine the impedance match condition, the spacing between the layers,  $\delta_z$ , is varied. The extracted parameters from these measurements at 50 MHz are shown in Figure 3. It was deduced from finite element method (FEM) numerical modelling<sup>16</sup> that 4 cubes in the propagation direction was the minimum number required for the cube arrays to act as a bulk structure as the addition of more cubes did not change the extracted effective material parameters to 1 decimal place. The predictions from FEM modelling, utilising the material parameters of the bulk ferrite composite from Figure 4, are also shown. It should be noted that the comparison of experiment with simulation is good considering the extreme sensitivity to  $\delta_z$  in the experiment. Any small variations in alignment of the cube array or spacer thickness will impact  $\epsilon'_{\text{eff}}$  and would lead to differences between the experimental  $\delta_z$  value and that used in the model predictions.

If one considers the polyester to be the low permittivity spacing layer, and the planar array of cubes to be the ferrite layer in Eqs. (2) and (3), then the expected strong dependence of  $\epsilon'_{\text{eff}}$  and relatively weak linear dependence of  $\mu'_{\text{eff}}$  on  $\delta_z$  is as observed. The experimental results suggest that the structured ferrite composite will have  $\epsilon'_{\text{eff}} = \mu'_{\text{eff}}$ , when  $\delta_z/2 = 1.15$  mm. (Note, the average  $\epsilon'_r$  for the ferrite composite is  $98 \pm 5$  (see Figure 4), hence  $\epsilon'_{\text{eff}}$  has an uncertainty associated with it, indicated by the dotted lines in Figure 5.) It must be noted that although the modelled values of  $\epsilon'_{\text{eff}}$  and  $\mu'_{\text{eff}}$  fall within the experimental uncertainties (excluding the single data point for  $\epsilon'_{\text{eff}}$  at  $\delta_z/2 = 0.75$  mm), neither can be accurately predicted by Eqs (2) and (3). Equations (2) and (3) provide exact values of  $\epsilon'_{\text{eff}}$  and  $\mu'_{\text{eff}}$  for an array of slabs of alternating values of permittivity and permeability which has been confirmed using FEM

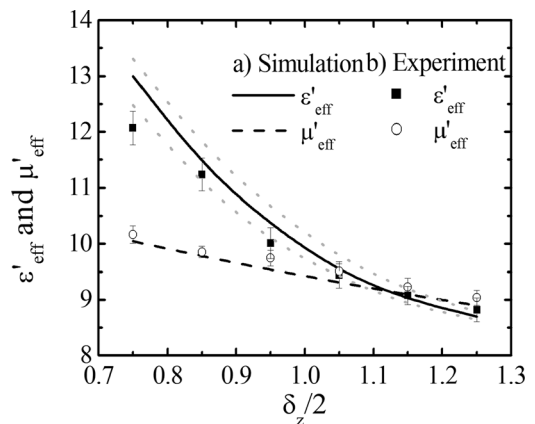


FIG. 5. Effect of varying the separation between the layers ( $\delta_z$ ) on the effective relative real permittivity ( $\epsilon'_{\text{eff}}$ ) and permeability ( $\mu'_{\text{eff}}$ ) for the anisotropic array of ferrite cubes at 50 MHz. (a) Predictions from FEM modelling with the uncertainty based on the range of  $\epsilon'_r$  values for the ferrite composite indicated by dotted lines, and (b) averaged experimental results and standard deviation.

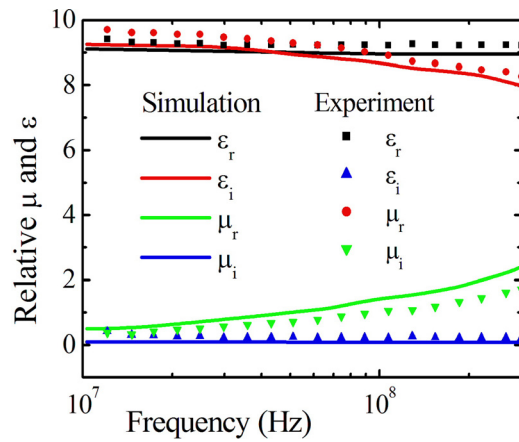


FIG. 6. FEM modelling (line) and experimental results (points) of the complex permeability and permittivity as a function of frequency for the impedance matched anisotropic array of ferrite cubes. The cube spacings are 0.1 mm in both the  $x$  and  $y$ -directions, with  $\delta_z/2 = 1.05$  mm in the  $z$ -direction (parallel to the incident electric field vector).

modelling, however, an analytical solution to predict the exact values of  $\epsilon'_{\text{eff}}$  and  $\mu'_{\text{eff}}$  for the array of cubes is not possible due to the conflicting boundary conditions, hence approximations can only be obtained.

Figure 6 shows the extracted value of  $\tilde{\mu}_{\text{eff}}$  and  $\tilde{\epsilon}_{\text{eff}}$  for the anisotropic impedance matched, cube array ( $\delta_z/2 = 1.05$  mm) when the electric field is in the  $z$ -direction. Predictions from the FEM model (line) and the experimental data (points) are shown. Note that while  $\mu'_{\text{eff}}$  and  $\epsilon'_{\text{eff}}$  for the experiment are equal to within 4% of the averaged values across the frequency range from 10 to 300 MHz,  $\mu'_{\text{eff}}$  and  $\epsilon'_{\text{eff}}$  remain small but are dispersive beyond 70 MHz. Above  $\sim 70$  MHz, an increase in  $\mu'_r$  is accompanied by an associated decrease in  $\mu'_i$ , due to the gyromagnetic spin resonance. As  $\mu'_{\text{eff}}$  and  $\epsilon'_{\text{eff}}$  are equal at a value of 9.5, the refractive index is also 9.5 from 10 to 300 MHz.

Figure 7 shows the experimentally measured reflected (black line) and transmitted (red line) intensity from the 1.05 mm spaced ferrite cube array as a function of frequency. For frequencies up to 70 MHz, the transmission remains above 95%, whilst the reflection remains at less than 0.3%. Above about 70 MHz, the transmission falls significantly due to losses associated with the magnetic resonance. In addition, our experimental results demonstrate that a 50 mm length of this structure maintains a reflection coefficient of less than 0.3% up to 300 MHz, despite becoming highly absorbing. Using simulations 22 layers of this structure (200 mm) in the propagation direction is the required thickness to absorb 97% of the radiation at 200 MHz (corresponding wavelength 1.5 m) making it an excellent absorber at higher frequencies.

In this study, a simple anisotropic array of ferrite cubes that provides a broadband, impedance matched structured ferrite composite from 10 to 70 MHz has been demonstrated. Despite having a refractive index of 9.5, the reflection, for one specific linear polarisation, from this structure is less than 0.3% over this frequency band. As a broadband impedance matched structure, this cube array is the first step in realising the material properties required to create transformation optics devices. It also presents potential for

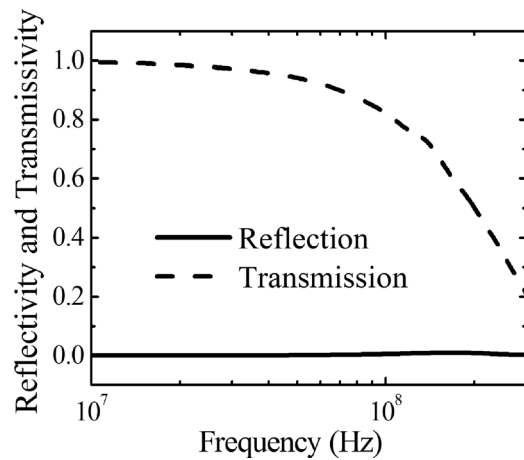


FIG. 7. Experimentally determined reflectivity and transmissivity from 1.05 mm spaced ferrite cube array with the incident electric field vector parallel to the  $z$ -axis.

exploitation as an electromagnetic absorber of sub-wavelength thickness. Although slabs of ferrite material (as opposed to cubes) with their slab normal parallel to the incident electric field direction would provide independent control of  $\epsilon'_{\text{eff}}$ , to simultaneously allow for control of  $\mu'_{\text{eff}}$  the slabs must be split in a direction parallel to the incident magnetic induction. Further investigations to overcome the limits of Snoek's law<sup>17</sup> will likely yield a ferrite material with a higher resonant frequency, and the prospect of a broader impedance matched region.

The authors wish to acknowledge the financial support of the EPSRC and DSTL for funding LP's Ph.D. studentship through the University of Exeter Doctorial Training account, J.R.S. and A.P.H. through the QUEST programme Grant (EP/I034548/1) "The Quest for Ultimate Electromagnetics using Spatial Transformations."

<sup>1</sup>H. Mosallaei and K. Sarabandi, *IEEE Trans. Antennas Propag.* **52**, 1558 (2004).

<sup>2</sup>A. Goldman, *Modern Ferrite Technology* (Van Nostrand Reinhold, Springer, 2010), p. 217.

<sup>3</sup>M. J. Iqbal, Z. Ahmad, T. Meydan, and Y. Melikhov, *J. Appl. Phys.* **111**, 033906 (2012).

<sup>4</sup>A. Thaker, A. Chevalier, J.-L. Mattei, and P. Queffelec, *J. Appl. Phys.* **108**, 014301 (2010).

<sup>5</sup>L. Kong, Z. Li, G. Lin, and Y. Gan, *IEEE Trans. Magn.* **43**, 6 (2007).

<sup>6</sup>H. Su, X. Tang, H. Zhang, Y. Jing, and F. Bai, *J. Appl. Phys.* **113**, 17B301 (2013).

<sup>7</sup>W. Zhang, Y. Bai, X. Han, L. Wanga, X. Lu, L. Qiao, J. Cao, and D. Guo, *Mater. Res. Bull.* **48**, 3850–3853 (2013).

<sup>8</sup>P. Alitalo, O. Luukkonen, J. Vehmas, and J. Tretyakov, *IEEE Antennas Wirel. Propag. Lett.* **7**, 187 (2008).

<sup>9</sup>N. Landy, S. Sajuyigbe, J. Mock, D. Smith, and W. Padilla, *Phys. Rev. Lett.* **100**, 207402 (2008).

<sup>10</sup>K. Kim and Q. Park, *Sci. Rep.* **3**, 1062 (2013).

<sup>11</sup>M. Matsumoto and Y. Miyata, *IEEE Trans. Magn.* **33**, 4459 (1997).

<sup>12</sup>L. Parke, I. Hooper, R. Hicken, C. Dancer, P. Grant, I. Youngs, A. Hibbins, and J. Sambles, *APL Mater.* **1**, 042108 (2013).

<sup>13</sup>A. Nicholson and G. Ross, *IEEE Trans. Instrum. Meas.* **19**, 377 (1970).

<sup>14</sup>W. W. Weir, *Proc. IEEE* **62**, 33 (1974).

<sup>15</sup>T. Tsutaoka, *J. Appl. Phys.* **93**, 2789 (2003).

<sup>16</sup>See <http://www.ansoft.com/products/hf/hfss/> for Ansoft Corporation, Ansoft HFSS, Pittsburgh, PA.

<sup>17</sup>J. Snoek, *Physica* **14**, 207 (1948).